

# Weierstraß-Institut für Angewandte Analysis und Stochastik

im Forschungsverbund Berlin e.V.

Preprint

ISSN 0946 – 8633

## On the Landau-Levich problem for non-Newtonian liquids

Konstantin Afanasiev<sup>2</sup>, Andreas Münch<sup>1</sup> and Barbara Wagner<sup>2</sup>

submitted: March 16, 2007

<sup>1</sup> Humboldt University of Berlin,  
Institute of Mathematics, D-10099 Berlin

<sup>2</sup> Weierstrass Institute for Applied Analysis and Stochastics (WIAS),  
Mohrenstraße 39, D-10117 Berlin

No. 1215  
Berlin 2007



---

2000 *Mathematics Subject Classification.* 34B15, 35G25, 35K55, 35Q35.

*Key words and phrases.* lubrication models, non-Newtonian flow, fluid dynamics, phase plane analysis.

Edited by  
Weierstraß-Institut für Angewandte Analysis und Stochastik (WIAS)  
Mohrenstraße 39  
10117 Berlin  
Germany

Fax: + 49 30 2044975  
E-Mail: [preprint@wias-berlin.de](mailto:preprint@wias-berlin.de)  
World Wide Web: <http://www.wias-berlin.de/>

## Abstract

In this paper the drag-out problem for shear-thinning liquids at variable inclination angle is considered. For this free boundary problem dimension-reduced lubrication equations are derived for the most commonly used viscosity models, namely, the power-law, Ellis and Carreau model. For the resulting lubrication models a system of ordinary differential equation governing the steady state solutions is obtained. Phase plane analysis is used to characterize the type of possible steady state solutions and their dependence on the rheological parameters.

## 1 Introduction

The drag-out problem, which is the problem of withdrawal of a plate or fiber from a liquid bath, is one of the fundamental problems in fluid mechanics and has many applications in nature and technology. The seminal paper on this problem was given by Landau and Levich [12] and systematic extensions can be found in [22], [17] and [21]. While the methods in these studies could be extended and used in various applications [15], [3], they focus on Newtonian liquids. However, many applications that are concerned with polymeric liquids and suspensions show nonlinear stress-strain relationships, see e.g. [6] and [16]. In fact, most polymer solutes used in coating exhibit some degree of shear-thinning behavior. Typically, they show distinct viscosity regimes when subject to shear stress. At very low shear rates they behave as a Newtonian fluid; as the shear rate increases the behavior starts to become nonlinear, after further increase it moves into a regime where the viscosity can be modeled by a power-law relation. Finally, at very high shear rates the behavior becomes Newtonian once more.

While most studies in coating flows were concerned with applications of spin coating, rimming flows or flows of films down an inclined plane, see e.g. [2], [4], [8], [10], [13], [14], [20], [9], we are interested in studying the relevant parameters that control the shape of the free boundary exhibited by shear-thinning liquids during the steady withdrawal from a reservoir. We choose for our studies some of the most commonly used viscosity models, which are the power-law, the Ellis and the Carreau-Yasuda model. A recent discussion on the suitability of these models for studying thin film flows of shear-thinning liquids is given in [19] for the case of flows in thin channels, i.e. surface tension is neglected. Here, we use asymptotic arguments to systematically derive from the underlying equations of conservation of momentum and mass, together with the boundary conditions of normal and tangential shear stress, the leading order equations. These can be integrated out to yield extended

lubrication models for the profile of the film that take account of surface tension and are also valid in the meniscus region.

In the following sections we are concerned with the steady states. For all three models we can derive a system of ordinary differential equations for the steady state solutions. A careful phase plane analysis then shows the existence of two types of solutions. Type I corresponding to a monotone film profile and Type II, corresponding to a spatially oscillating film profile. We develop criteria for the power-law and Ellis model that select the type of solution. Another difference between these solution is also the thickness of the films towards the uniform region far away from the meniscus and is being discussed in a separate section where matched asymptotic solutions and numerical solutions are compared.

## 2 Problem formulation

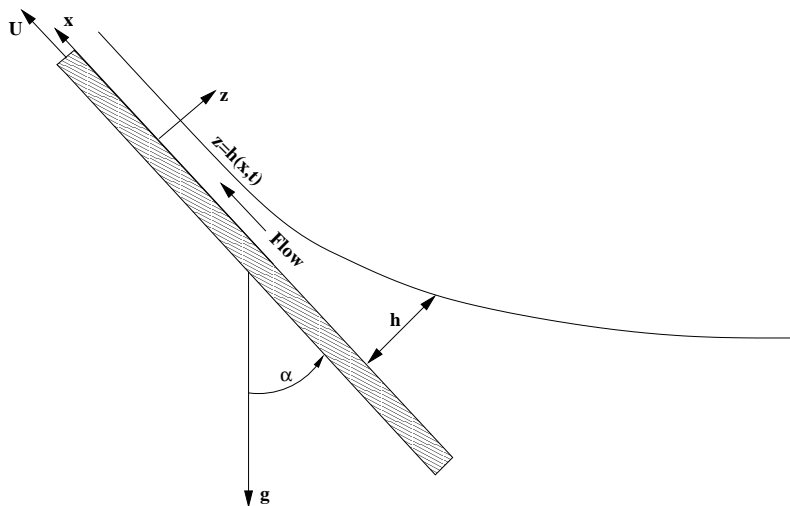


Figure 1: Thin film withdrawn at an angle  $\alpha$  from a liquid reservoir.

We consider the evolution of a thin layer of non-Newtonian shear-thinning liquid on the inclined plane that can be withdrawn from a bath with velocity  $U$ , see figure 1, or pushed into a bath with velocity  $-U$ , at the angle  $\alpha$  with the horizontal axis. Here, we only consider the two-dimensional case where the solution is independent of the coordinate  $\bar{y}$  and the thickness of the film is denoted by  $\bar{h}(\bar{x}, \bar{t})$ . As usual,  $\bar{x}$  and  $\bar{z}$  denote the axes in stream-wise and cross-stream directions, respectively.

The balance laws for momentum and mass of an incompressible fluid of density  $\rho$  in the presence of gravity are

$$\rho \frac{d\bar{u}}{d\bar{t}} = -\bar{p}_{\bar{x}} - \bar{\tau}_{\bar{x}}^{xx} - \bar{\tau}_{\bar{z}}^{zx} - \rho g \cos \alpha, \quad (2.1a)$$

$$\rho \frac{d\bar{w}}{d\bar{t}} = -\bar{p}_{\bar{z}} - \bar{\tau}_{\bar{x}}^{xz} - \bar{\tau}_{\bar{z}}^{zz} - \rho g \sin \alpha, \quad (2.1b)$$

$$\bar{u}_{\bar{x}} + \bar{w}_{\bar{z}} = 0. \quad (2.1c)$$

for  $0 < \bar{z} < \bar{h}$  and  $-\infty < \bar{x} < +\infty$ . Here, we denote  $d/dt = \partial_t + u\partial_x + w\partial_z$ . At the free surface  $\bar{z} = \bar{h}$  we have the normal and tangential stress condition

$$\frac{\bar{\tau}^{zz} - 2\bar{\tau}^{xz}\bar{h}_{\bar{x}} + \bar{\tau}^{xx}\bar{h}_{\bar{x}}^2}{1 + \bar{h}_{\bar{x}}^2} - \bar{p} = \sigma\bar{\kappa}, \quad (2.1d)$$

$$(\bar{\tau}^{\bar{z}\bar{z}} - \bar{\tau}^{xx})\bar{h}_{\bar{x}} + \bar{\tau}^{xz}(1 - \bar{h}_{\bar{x}}^2) = 0, \quad (2.1e)$$

respectively. At the surface of the plane  $\bar{z} = 0$  we require the no-slip condition and impermeability of the plane, i.e.

$$\bar{u} = U, \quad \bar{w} = 0 \quad (2.1f)$$

where  $\bar{u}(\bar{x}, \bar{z}, \bar{t})$ ,  $\bar{w}(\bar{x}, \bar{z}, \bar{t})$  denote the fluid velocity vector components,  $\underline{\tau}$  is the shear stress tensor

$$\underline{\tau} = \begin{pmatrix} \bar{\tau}^{xx} & \bar{\tau}^{xz} \\ \bar{\tau}^{zx} & \bar{\tau}^{zz} \end{pmatrix}, \quad \dot{\underline{\gamma}} = \begin{pmatrix} 2\bar{u}_{\bar{x}} & \bar{u}_{\bar{z}} + \bar{w}_{\bar{x}} \\ \bar{u}_{\bar{z}} + \bar{w}_{\bar{x}} & 2\bar{w}_{\bar{z}} \end{pmatrix}$$

which is related to the strain tensor via

$$\underline{\tau} = -\eta\dot{\underline{\gamma}}. \quad (2.2)$$

We denote by  $\eta$  the viscosity and  $\dot{\underline{\gamma}}$  is the strain rate,

$$\dot{\underline{\gamma}} = (2\bar{u}_{\bar{x}}^2 + \bar{u}_{\bar{z}}^2 + 2\bar{u}_{\bar{z}}\bar{w}_{\bar{x}} + \bar{w}_{\bar{x}}^2 + 2\bar{w}_{\bar{z}}^2)^{\frac{1}{2}}. \quad (2.3)$$

Additionally we include, in particular for the cases of vertical drag-out, the nonlinear curvature at the free boundary  $\bar{h}(\bar{x}, \bar{t})$

$$\bar{\kappa} = \frac{\bar{h}_{\bar{x}\bar{x}}}{(1 + \bar{h}_{\bar{x}}^2)^{3/2}}. \quad (2.4)$$

For a discussion of the importance of this modification see e.g. [17] and [22].

Some of the most well-known viscosity models for shear-thinning or shear-thickening fluids are: the power-law model

$$\eta = m\dot{\underline{\gamma}}^{n-1} \quad (2.5)$$

that is pseudoplastic or shear thinning for  $n < 1$  and shear thickening if  $n > 1$ , the Ellis model, given by

$$\frac{\eta_0}{\eta} = 1 + \left| \frac{\tau}{\tau_{1/2}} \right|^{q-1} \quad (2.6)$$

where  $\eta_0$  denotes the viscosity at zero shear and  $\tau_{1/2}$  is the value at which  $\eta = \eta_0/2$  and the Carreau-Yasuda Model

$$\frac{\eta - \eta_\infty}{\eta_0 - \eta_\infty} = (1 + (\lambda\dot{\underline{\gamma}})^c)^{(k-1)/c} \quad (2.7)$$

where  $\eta_0$  and  $\eta_\infty$  are the limiting viscosities at low and high shear rates, respectively. We note that, unlike the Ellis and Carreau-Yasuda models, the

power-law model is only meant to apply at large shear rates. While the Ellis model may for certain liquids underpredict the viscosity in the low shear transition region from power law to Newtonian behavior, the results in [19] show that in many cases it compares well with the results for the Carreau-Yasuda model, which is most commonly employed for industrial applications. The main advantage of the Ellis model over Carreau-Yasuda is that, in the case of a film with a free surface, an explicit expression for the film profile may be derived. Nevertheless, we show here, that for the case of  $\eta_\infty = 0$  and  $c = 2$ , i.e. the so-called Carreau model, we still can derive a dimension-reduced lubrication model.

In the following section we derive the lubrication equations for these models for the drag-out problem. We will take account of the nonlinear curvature which will be important when  $\alpha$  is small, or even zero for the case of vertical drag-out.

### 3 Lubrication models for power-law, Ellis and Carreau model

To begin with, we introduce dimensionless variables

$$\begin{aligned}\bar{x} &= L x, & \bar{u} &= U u, & \bar{p} &= P p, & \bar{h} &= H h, \\ \bar{z} &= H z, & \bar{w} &= W w, & \bar{t} &= T t,\end{aligned}$$

and assume that

$$\frac{U}{L} = \frac{1}{T}, \quad \text{and} \quad \varepsilon = \frac{H}{L} \ll 1.$$

For the power-law model we observe first that the strain rate is

$$\bar{\dot{\gamma}} = \frac{U}{H} \dot{\gamma}, \quad \dot{\gamma} = (2\varepsilon^2 u_x^2 + u_z^2 + 2\varepsilon^2 u_z w_x + \varepsilon^4 w_x^2 + 2\varepsilon^2 w_z^2)^{\frac{1}{2}}$$

and the shear stress components are

$$\begin{aligned}\bar{\tau}^{xx} &= -\frac{m U^n}{H^n} \varepsilon 2u_x \dot{\gamma}^{n-1}, & \bar{\tau}^{xz} &= -\frac{m U^n}{H^n} (u_z + \varepsilon^2 w_x) \dot{\gamma}^{n-1}, \\ \bar{\tau}^{zz} &= -\frac{m U^n}{H^n} 2\varepsilon w_z \dot{\gamma}^{n-1}, & \bar{\tau}_{\bar{x}}^{xx} &= -\frac{m U^n}{H^{n+1}} \varepsilon^2 (2u_x \dot{\gamma}^{n-1})_x, \\ \bar{\tau}_{\bar{z}}^{xz} &= -\frac{m U^n}{H^{n+1}} [(u_z + \varepsilon^2 w_x) \dot{\gamma}^{n-1}]_z, & \bar{\tau}_{\bar{z}}^{zz} &= -\frac{m U^n}{H^{n+1}} \varepsilon (2w_z \dot{\gamma}^{n-1})_z, \\ \bar{\tau}_{\bar{x}}^{xz} &= -\frac{m U^n}{H^{n+1}} \varepsilon [(u_z + \varepsilon^2 w_x) \dot{\gamma}^{n-1}]_x.\end{aligned}$$

As usual, the characteristic scale for the pressure is obtained by balancing the  $x$ -momentum equation (2.1a)  $p_x$  with the dominant viscous stress term  $\tau_z^{xz}$  then

$$P = \frac{m U^n}{\varepsilon H^n}. \quad (3.1)$$

Requiring the balance of the normal pressure and surface tension at the free surface yields

$$P = \frac{\sigma \varepsilon^2}{H}. \quad (3.2)$$

This in turn yields for the capillary number

$$Ca = \frac{\eta U}{\sigma} = \frac{mU^{n-1}U}{H^{n-1}\sigma} = \frac{mU^n}{H^{n-1}\sigma} = \varepsilon^3 \quad (3.3)$$

Balancing  $\tau_z^{xz}$  in equation (2.1a) with the gravity term yields an expression for the characteristic height

$$H = \left( \frac{mU^n}{\rho g \cos \alpha} \right)^{\frac{1}{n+1}} \quad (3.4)$$

Hence, we obtain for the dimensionless governing equations

$$\varepsilon^4 Re \frac{du}{dt} = -p_x + \varepsilon^2 (2u_x \dot{\gamma}^{n-1})_x + [(u_z + \varepsilon w_x) \dot{\gamma}^{n-1}]_z - 1, \quad (3.5a)$$

$$\varepsilon^6 Re \frac{dw}{dt} = -p_z + \varepsilon^2 [(u_z + \varepsilon^2 w_x) \dot{\gamma}^{n-1}]_x + \varepsilon^2 (2w_z \dot{\gamma}^{n-1})_z - D, \quad (3.5b)$$

$$u_x + w_z = 0, \quad (3.5c)$$

for  $0 < z < h(x, t)$  and  $-\infty < x < +\infty$ . At the free boundary  $z = h$  we find now

$$p = -\frac{h_{xx}}{(1 + \varepsilon^2 h_x^2)^{3/2}} + \varepsilon^2 \frac{2[w_z - (u_z + \varepsilon^2 w_x)h_x + \varepsilon^2 u_x h_x^2] \dot{\gamma}^{n-1}}{1 + \varepsilon^2 h_x^2} \quad (3.5d)$$

$$0 = 2\varepsilon^2 (w_z - u_x)h_x + (u_z + \varepsilon^2 w_x)(1 - \varepsilon^2 h_x^2) \quad (3.5e)$$

and at the surface of the plate  $z = 0$  we have

$$u = 1, \quad w = 0. \quad (3.5f)$$

The dependence on the inclination angle is now contained in the parameter

$$D = \varepsilon \tan \alpha. \quad (3.5g)$$

To leading order in  $\varepsilon$  we find  $\tau^{xz} = -u_z |u_z|^{n-1}$  and obtain the following free boundary problem

$$0 = -p_x - \tau_z^{xz} - 1, \quad (3.6a)$$

$$0 = -p_z - D, \quad (3.6b)$$

$$0 = u_x + w_z. \quad (3.6c)$$

with boundary conditions

$$u = 1, \quad w = 0, \quad \text{at } z = 0 \quad (3.7a)$$

$$u_z = 0, \quad p = -\kappa, \quad \text{at } z = h(x). \quad (3.7b)$$

This problem can now be integrated to yield a single partial differential equation for the profile  $h(x, t)$ . We obtain first the pressure by integrating (3.6b) with respect to  $z$  from  $z$  to  $h$  and use the boundary condition (3.7b)

$$p = -\kappa + D(h - z) \quad (3.8)$$

From the leading order equation (3.6a) we can get

$$(u_z |u_z|^{n-1})_z = -(\kappa_x - Dh_x - 1) \quad (3.9)$$

and intergrating this from  $z$  to  $h(x, t)$  and noting that  $z \leq h(x, t)$

$$u_z = |\psi|^{\frac{1-n}{n}} \psi (h - z)^{\frac{1}{n}} \quad (3.10)$$

where

$$\psi = \kappa_x - Dh_x - 1 \quad (3.11)$$

We integrate this equation once more from 0 to  $z$  and use the no-slip condition to get for the velocity

$$u(z) = 1 - \frac{n}{n+1} |\psi|^{\frac{1-n}{n}} \psi \left( (h - z)^{\frac{n+1}{n}} - h^{\frac{n+1}{n}} \right). \quad (3.12)$$

This can now be used in the kinematic conditon at the free boundary

$$\partial_t h = -\partial_x \int_0^h u dz \quad (3.13)$$

to obtain

$$\partial_t h = -\partial_x \left[ h - |\psi|^{\frac{1-n}{n}} \psi \frac{n}{n+1} \left( \frac{n}{2n+1} h^{\frac{2n+1}{n}} - h^{\frac{2n+1}{n}} \right) \right], \quad (3.14)$$

or, introducing the new time scale  $t \rightarrow \frac{2n+1}{n} t$  we get the following lubrication equation for the power-law model

$$\partial_t h = -\partial_x \left[ h^{\frac{2n+1}{n}} |\psi|^{\frac{1-n}{n}} \psi + \frac{2n+1}{n} h \right] \quad (3.15)$$

with boundary conditions

$$\lim_{x \rightarrow \infty} h = h_\infty, \quad \lim_{x \rightarrow \infty} h_x = 0, \quad (3.16a)$$

$$\lim_{x \rightarrow -\infty} \kappa = 0, \quad \lim_{x \rightarrow -\infty} h = \infty \quad . \quad (3.16b)$$

In principle, the derivation of the lubrication approximation for the Ellis- and Carreau-Yasuda model are quite similar as demonstrated above. We therefore state only the main differences here and refer for details to the corresponding appendices.

For the Ellis model the balance in the  $x$ -momentum equation of  $p_x$  with the dominant viscous stress term  $\tau_z^{xz}$  now yields the following characteristic scale for the pressure

$$P = \frac{\eta_0 U}{2\varepsilon H} \quad (3.17)$$



Similarly, balancing  $\tau_z^{xz}$  in  $x$ -momentum equation with the gravity term gives the following characteristic height

$$H = \left( \frac{\eta_0 U}{2\rho g \cos \alpha} \right)^{\frac{1}{2}} \quad (3.18)$$

Here,  $\eta_0$ , the viscosity at zero shear, is used to non-dimensionalize the viscosity

$$\bar{\eta} = \frac{\eta_0}{2} \eta \quad (3.19)$$

where

$$\frac{\eta_0}{\bar{\eta}} = 1 + \left| \frac{\bar{\tau}}{\tau_{1/2}} \right|^{q-1} \quad (3.20)$$

and hence

$$\frac{2}{\eta} = 1 + E^{1-q} |\tau^{xz}|^{q-1}. \quad (3.21)$$

with

$$E = \frac{2H\tau_{1/2}}{\eta_0 U}. \quad (3.22)$$

The resulting non-dimensional equations can now be integrated, resulting in the following expression for the velocity

$$u = \frac{1}{2} \left[ \psi(hz - z^2) + \frac{\psi|\psi|^{q-1}}{E^{q-1}} \left( \frac{-1}{q+1} (h-z)^{q+1} + \frac{1}{q+1} h^{q+1} \right) \right] + 1 \quad (3.23)$$

from which we obtain, after rescaling time as  $t \rightarrow 3t$ , from the kinematic condition the lubrication equation for the Ellis model

$$\partial_t h = -\partial_x \left[ \frac{1}{2} \left( \psi h^3 + \frac{3}{q+2} \frac{1}{E^{q-1}} \psi |\psi|^{q-1} h^{q+2} \right) + 3h \right] \quad (3.24)$$

together with the boundary conditions (3.16).

Finally, for the Carreau-Yasuda model note first that the parameter  $\lambda$  is assumed to be of order  $O(1/\varepsilon)$ , i.e.

$$\bar{\lambda} = \lambda T = \lambda^* \varepsilon T \quad (3.25)$$

where  $\lambda^* = O(1)$ . If  $\lambda$  would be of larger or smaller order the lubrication scaling we consider below would simplify into the lubrication problem for the power-law or Newtonian case, respectively. Additionally, we set  $\eta_\infty = 0$  for simplicity.

Hence, we have

$$\eta = \eta_0 [1 + (\lambda^* \dot{\gamma})^c]^{\frac{k-1}{c}} \quad (3.26)$$

and the shear stress components are

$$\begin{aligned} \bar{\tau}^{xx} &= -\frac{\eta_0 U}{H} \varepsilon^2 u_x [1 + (\lambda \dot{\gamma})^c]^{\frac{k-1}{c}}, \\ \bar{\tau}^{xz} &= -\frac{\eta_0 U}{H} (u_z + \varepsilon^2 w_x) [1 + (\lambda \dot{\gamma})^c]^{\frac{k-1}{c}}, \\ \bar{\tau}^{zz} &= -\frac{\eta_0 U}{H} \varepsilon^2 2 w_z [1 + (\lambda \dot{\gamma})^c]^{\frac{k-1}{c}}, \end{aligned}$$

Integrating the system (3.6a)-(3.7b) once w.r.t.  $z$  we find

$$u_z (1 + |\lambda^* u_z|^c)^{\frac{k-1}{c}} = \psi(x, t)(h - z) \quad (3.27)$$

As shown in appendix 2, one can find for the velocity  $u$  the representation

$$u(x, z, t) = -\frac{F(\omega(g(z))) - F(\omega(g(0)))}{c\lambda^{*2}\psi} + 1 \quad (3.28)$$

where

$$F(\omega) = \int \frac{\omega^{\frac{2-c}{c}}(1+k\omega)}{(1+\omega)^{\frac{1-k}{c}+1}} d\omega \quad (3.29)$$

can be written in terms of generalized hypergeometric functions, and where  $\omega$  and  $g$  are related by

$$\omega(1+\omega)^{k-1} = g(x, z, t), \quad \text{with } g := (\lambda^*|\psi|(h-z))^c \quad (3.30)$$

Furthermore, for the Carreau model, i.e.  $c = 2$ , one can integrate once more to obtain a representation for the flux

$$\begin{aligned} Q^C(x, t) &= \int_0^h u dz \quad (3.31) \\ &= \frac{\sqrt{\omega_0}}{\lambda^{*3}(k+1)\psi|\psi|} \left[ \frac{k\omega_0 - 1}{(\omega_0 + 1)^{\frac{1-k}{2}}} \left( F_1 + \frac{k\omega_0}{3} F_2 \right) + \left( F_3 - \frac{k^2\omega_0^2}{5} F_4 \right) \right] + h \end{aligned}$$

and hence the corresponding lubrication equation

$$\partial_t h = -\partial_x Q^C \quad (3.32)$$

where the  $F_i$  denote the following generalized hypergeometric functions, see e.g. [1],

$$F_1 = F\left(\frac{1}{2}, \frac{3-k}{2}; \frac{3}{2}; -\omega_0\right), \quad F_2 = F\left(\frac{3-k}{2}, \frac{3}{2}; \frac{5}{2}; -\omega_0\right), \quad (3.33)$$

$$F_3 = F\left(\frac{1}{2}, 2-k; \frac{3}{2}; -\omega_0\right), \quad F_4 = F\left(\frac{5}{2}, 2-k; \frac{7}{2}; -\omega_0\right) \quad (3.34)$$

and

$$w_0 = w(g(0)),$$

together with the boundary conditions (3.16) at  $x \rightarrow \pm\infty$ . We next investigate the steady state solutions for these models.

## 4 Steady states

### 4.1 Power-law, Ellis and Carreau model

Set  $\partial_t h = 0$  in (3.15) and integrate w.r.t.  $x$  using the boundary conditions (3.16), to obtain for the flux at  $+\infty$ . For convenience set

$$a = \frac{2n+1}{n}, \quad \text{and} \quad b = \frac{1-n}{n}. \quad (4.1)$$

Then we have

$$h^a \psi |\psi|^b + ah = Q_\infty^{PL} \quad (4.2)$$

where the flux at  $+\infty$  is

$$Q_\infty^{PL} = ah_\infty - h_\infty^a \quad (4.3)$$

Note now, that in the case of a power-law viscosity we can obtain an explicit expression for  $\psi$  as a function of  $h$ . Let us denote it with

$$\psi^{PL} = \frac{(Q_\infty^{PL} - ah) |Q_\infty^{PL} - ah|^{n-1}}{h^{2n+1}} \quad (4.4)$$

Therefore, we obtain the following third order ODE for the steady states

$$\left( \frac{h_{xx}}{(1 + \varepsilon^2 h_x^2)^{3/2}} \right)_x = 1 + Dh_x + \psi^{PL} \quad (4.5)$$

We solve this ODE by first writing it as a system of first order equations. For this we note first that, if we define

$$\gamma(x) = \frac{h_x}{\sqrt{1 + \varepsilon^2 h_x^2}} \quad (4.6)$$

then  $\gamma_x = \kappa$ . Hence, the system can be written as

$$h_x = \frac{\gamma}{\sqrt{1 - \varepsilon^2 \gamma^2}} \quad (4.7)$$

$$\gamma_x = \kappa \quad (4.8)$$

$$\kappa_x = 1 + \frac{D\gamma}{\sqrt{1 - \varepsilon^2 \gamma^2}} + \psi^{PL} \quad (4.9)$$

as long as  $\varepsilon|\gamma| < 1$ . The boundary conditions are

$$h \rightarrow h_\infty, \quad \gamma \rightarrow 0, \quad \kappa \rightarrow 0 \quad \text{as } x \rightarrow \infty, \quad (4.10a)$$

i.e. towards the flat film, and

$$h \rightarrow \infty, \quad \gamma \rightarrow -1/\varepsilon, \quad \kappa \rightarrow 0 \quad \text{as } x \rightarrow 0, \quad (4.10b)$$

that is, towards the reservoir. The conditions in the thin flat film are  $h = h_\infty$ ,  $\gamma = 0$  (since  $h_x = 0$ ) and  $\kappa = 0$  as  $x \rightarrow \infty$ .

For the Ellis model we solve the same first order system (4.7)-(4.9), except that now  $\psi^{PL}$  is replaced by  $\psi^E$  in (4.9). Now,  $\psi^E$  is the solution of

$$\frac{\psi^E}{2} \left[ 1 + \frac{3}{q+2} \left( \frac{h}{E} \right)^{q-1} |\psi^E|^{q-1} \right] h^3 + 3h = Q_\infty^E \quad (4.11)$$

where

$$Q_\infty^E = 3h_\infty - \frac{1}{2} \left[ 1 + \frac{3}{q+2} \left( \frac{h_\infty}{E} \right)^{q-1} \right] h_\infty^3 \quad (4.12)$$

For the Carreau model  $\psi^{PL}$  is replaced by  $\psi^C$ , which is the solution of

$$Q^C(x, t) = Q_\infty^C \quad (4.13)$$

where  $Q_\infty^C$  is given by

$$Q_\infty^C = h_\infty - \frac{\sqrt{\omega_\infty}}{\lambda^{*3}(k+1)} \left[ \frac{k\omega_\infty - 1}{(\omega_\infty + 1)^{\frac{1-k}{2}}} \left( F_1 + \frac{k\omega_\infty}{3} F_2 \right) + \left( F_3 - \frac{k^2\omega_\infty^2}{5} F_4 \right) \right] \quad (4.14)$$

The functions  $F_i$  are as in (3.33), (3.34) but for the argument  $\omega_\infty$  instead of  $\omega_0$ , where  $\omega_\infty$  is the solution of

$$\omega_\infty (1 + \omega_\infty)^{k-1} = (\lambda^* h_\infty)^2. \quad (4.15)$$

## 4.2 Classification of Type I/Type II solutions

We now discuss the possibility of steady state meniscus in more detail, i.e. of solutions of the system (4.7)-(4.9) which satisfy the required boundary conditions at zero and infinity, see (3.16). For simplicity, we focus first only on the power-law fluid, and later explain how the results carry over to the other types of fluids considered in this paper.

For a given value of  $Q_\infty$ , the ODE system typically has two equilibria,  $B = (h_B, 0, 0)$  and  $T = (h_T, 0, 0)$ , each of which can serve as the right far field state for the meniscus solution. Specifically, for  $0 < Q_\infty < a - 1$ , the two values  $h_B < h_T$  are the two solutions of the equation

$$ah_I - h_I^a = Q_\infty, \quad I \in \{B, T\}.$$

One easily finds that these solutions satisfy  $0 < h_B < 1 < h_T$ .

The trajectory of a meniscus solution must lie on the stable manifold of either  $B$  or  $T$ . Linearising (4.7)-(4.9) near  $I = B$  or  $I = T$  yields the system

$$(h, \gamma, \kappa)' = J_I(h, \gamma, \kappa),$$

where  $J_I$  is the Jacobian for the right hand side of (4.7)-(4.9), i.e.

$$J_I = \begin{pmatrix} 0 & 1 & 0 \\ 0 & 0 & 1 \\ r^{PL} & 0 & 0 \end{pmatrix}, \quad (4.16)$$

where

$$r_I^{PL} = \frac{2n+1}{h_I} (1 - h_I^{1-a}). \quad (4.17)$$

The eigenvalues of  $J_I$  are the solutions of

$$\lambda^3 = r_I^{PL}. \quad (4.18)$$

If  $r_I^{PL} < 0$ , then we have one negative real eigenvalue and a pair of complex conjugate eigenvalues with positive real part. In this case, the corresponding fixed point has a one-dimensional stable manifold. Conversely, if  $r_I^{PL} > 0$ , the fixed point has a two-dimensional stable manifold.

From the definition of  $a$ , we have  $a - 1 = (n + 1)/n > 0$ . Hence, we find that  $r_I^{PL} < 0$  if and only if  $h_I < 1$ , i.e. for the lower fix point,  $h_I = h_B$ . Trajectories that connect to this fixed point as  $x \rightarrow \infty$  must therefore be

identical with one of the two branches of the one-dimensional stable manifold  $W^s(B)$ . Conversely, for the top equilibrium, trajectories must lie on the two-dimensional stable manifold  $W^s(T)$ . Due to the pair of complex eigenvalues,  $h(x)$  will go through an infinite sequence of decaying oscillations as the trajectory approaches  $T$ . Following Münch and Evans [18], we distinguish meniscus solutions by the equilibrium they connect to: Solutions with trajectories that lie on  $W^s(B)$  are called Type I meniscus solutions, while those which connect to  $T$  are called Type II solutions.

To complete this discussion, we also need to characterize the trajectories that satisfy the boundary condition at  $x \rightarrow 0$ . Note that it is sufficient to find solutions for which  $h$  blows up as  $x$  approaches any finite value of  $x$  and  $\kappa$  goes to zero; since the system of ordinary differential equations (4.7)-(4.9) is autonomous, the singularity can always be shifted to zero.

If  $h$  and  $h_x$  blow-up, the dominant term on the left hand side of (4.5) is  $[h_{xx}/\epsilon^3 h_x^3]_x$ , and  $-1$  on the right. To capture the leading behavior of  $h$  as  $x \rightarrow 0$ , we can either choose to balance the two or assume that the left hand side vanishes to leading order. It turns out that the latter case leads to a bounded solution, and can be ruled out. Furthermore, by enforcing the balance and integrating up, one obtains that the only possibility for blow-up is

$$h(x) \sim -\epsilon^{-3/2} \ln x + c, \quad \text{for } x \rightarrow 0, \quad (4.19)$$

where  $c$  is an arbitrary constant. This also fixes the behaviour of  $\gamma$  and  $\kappa$ : we can conclude that

$$\gamma(x) \sim -\frac{1}{\epsilon} + \frac{1}{2}x^2, \quad \text{and } \kappa(x) \sim x, \quad \text{as } x \rightarrow 0. \quad (4.20)$$

The presence of a free constant in (4.19) suggests that the boundary condition imposed on  $h$  at the reservoir i.e. at  $x \rightarrow 0$  restrict the possible solutions to a two-dimensional manifold of trajectories, which we denote by  $W^0$ . Then, Type I meniscus solutions arise from a codimension-1 intersection of  $W^0$  and  $W^s(B)$ , which generically break under perturbations of the parameters, in particular, if  $Q_\infty$  hence  $h_B$  are changed with the other parameters held fixed. We therefore expect that Type I solutions will only exist for certain discrete far field film thicknesses  $h_B$  and flow rates  $Q_\infty$ . In fact, numerical evidence suggests that there is at most one value for  $Q_\infty$  and one Type I meniscus solution. On the other hand, intersections of  $W^0$  and  $W^s(T)$  have codimension 0 and therefore generically persist under perturbations. Thus, for Type II solutions, we expect that the film thickness can be varied continuously.

We can now explore the situation in phase space systematically by computing the two branches of  $W^s(B)$  and sufficiently densely spaced orbits on  $W^s(T)$  and  $W^0$ , using a numerical integrator (LSODE [11]). The initial values for  $W^s(B)$  and  $W^s(T)$  were obtained from the eigenspaces of  $J_I$  and the integration carried out in the direction of decreasing  $x$ , and from (4.19), (4.20) for  $W^0$ , for which the integration was carried out forward in  $x$ .

In fig. 2, we show the intersections of the trajectories with the Poincaré-Plane  $P = \{(h, \gamma, \kappa); h = 3.0\}$ . The values we chose were  $n = 1$ , i.e., the Newtonian case of the power law model,  $\epsilon = 1$  and  $Q_\infty$  was the value for which a Type I solution arises. This can be seen from the fact that the box

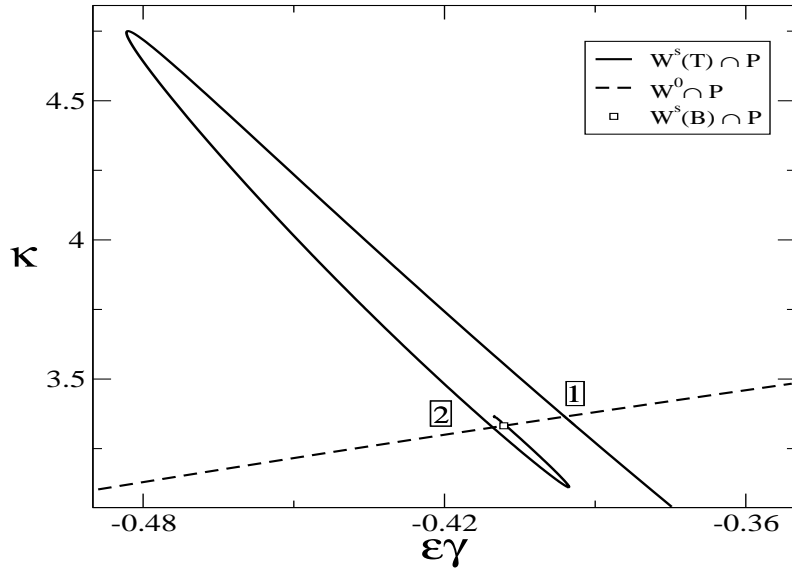


Figure 2: Poincaré section of the invariant manifolds with the plane  $P = \{(h, \gamma, \kappa); h = 3.0\}$ , obtained numerically for the Newtonian case of the power-law model, i.e. with  $n$  set to one, and with  $\epsilon = 0.1$ .

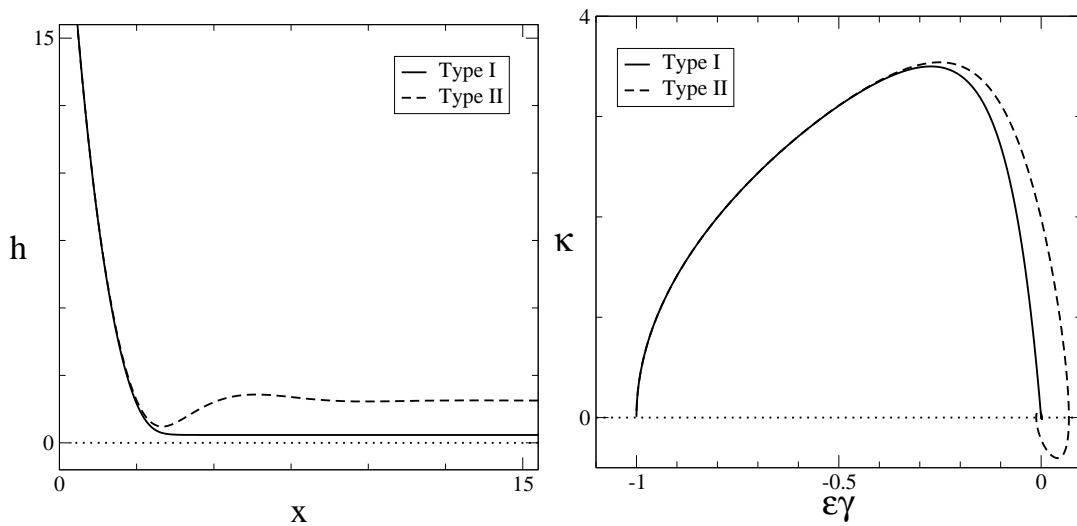


Figure 3: (a) Profiles of the Type I meniscus solution corresponding to the center of the spiral in figure 2, and of one of the Type II solutions, corresponding to the intersection of  $W^s(B)$  and  $W^s(T)$  with  $P$  labelled “1” in figure 2. (b) Projections of the trajectories for these two solutions onto the  $\epsilon\gamma$ - $\kappa$ -plane.

which marks the point where  $W^s(B)$  intersects the Poincaré-plane lies on top of  $W^0 \cap P$ , indicating that there is the corresponding trajectory satisfies all required boundary conditions at  $x \rightarrow 0$  and at  $x \rightarrow \infty$ .

Clearly visible is also the spiral structure in  $W^s(T) \cap P$ . This spiral arises for very similar reasons as in the phase space diagrams discussed for traveling wave solutions of Marangoni-gravity driven films [5] and menisci [18]. Briefly explained, it arises because trajectories on  $W^s(T)$  that pass close to  $B$  are “warped” around  $W^s(B)$  due to the presence of the two unstable complex conjugate eigenvalues of the linearised ODE system near  $B$ , thus forming a spiral structure with an infinite windings and  $W^s(B)$  located at its center. Since the latter lies on top of  $W^0$ , we expect an infinite number of intersections of  $W^s(T) \cap P$  and  $W^0 \cap P$ , each of which give rise to a different Type II solution. Only the first two of these intersections are distinguishable in figure 2.

Profiles of the Type I solution and the Type II solution corresponding to the intersection of  $W^s(T) \cap P$  and  $W^0 \cap P$  labelled on in figure 2 are shown in the next figure, figure 3 (a). While the Type I solution decays monotonely onto the flat film thickness  $h_\infty = h_B$  at  $x \rightarrow \infty$ , the Type II solution has a typically ‘dip’ near close to where it connects to the reservoir, and then decays through an infinite sequence of oscillations onto  $h_\infty = h_T$ . It is also instructive to look at projections of the trajectories of these two solutions onto the  $\epsilon\gamma$ - $\kappa$ -plane, shown in figure 3 (b). Both curves connect to the origin at  $x \rightarrow \infty$ , and to  $(-1, 0)$  at  $x \rightarrow 0$ , as required by the boundary conditions in (4.10). While for the curve for the Type I solution,  $\gamma$  behaves monotonely (as function of the arclength), the Type II curve has a spiral near the origin, arising from the oscillatory decay onto the flat film at  $x \rightarrow \infty$ .

Most of these derivations carry over for the Ellis mode. Basically,  $r^{PL}$  has to be replaced by the appropriate expression  $r^E$  in (4.16) and subsequent equations, which turns out to be

$$r^E = \frac{3}{1 + \frac{3q}{q+2} \left(\frac{h_\infty}{E}\right)^{q-1}} \left( \frac{1 + \left(\frac{h_\infty}{E}\right)^{q-1}}{h_\infty} - \frac{2}{h_\infty^3} \right) \quad (4.21)$$

Again, the sign of this expression determines the properties of the eigenvalues of the linearised ODE system, and we find the same situation: A single real negative eigenvalue for the lower fix point  $B$  and a complex conjugate pair with negative real part for  $T$ . Also, the situation for  $W^0$  and in particular its dimension remains the same. Hence, the codimension of the intersections of invariant manifolds that give rise to Type I and Type II solutions are as they were for the power-law model.

However, the upper bound for  $h_B$ , which is also the lower bound for  $h_T$ , is no longer one, but depends on  $E$ ; denote it by  $\bar{h}(E)$ . It is given by the solution of

$$\frac{\bar{h}(E)^2}{2} \left[ 1 + \left( \frac{\bar{h}(E)}{E} \right)^{q-1} \right] = 1. \quad (4.22)$$

Note that this bound on  $h_B$  and  $h_T$  delimits the range from above and below for the flat film thickness of the Type I and Type II meniscus solutions. In particular, the flat film thickness  $h_\infty = h_B$  for Type I solutions must lie in the

intervall from 0 to  $\bar{h}(E)$ . Noting that the Ellis model is only used for shear thinning liquids,  $q > 1$ , we find that for  $E \rightarrow 0$  this bound shrinks to zero. Conversely, for large  $E \rightarrow \infty$ , we obtain  $\bar{h}(E) \rightarrow \sqrt{2} > 1$ . This means that the type of solution may also be influenced by the shear stress  $\tau_{1/2}$  far upstream.

## 5 Film thickness

### 5.1 Asymptotic analysis

The film thickness  $h_\infty$  that is attained in steady state can be found easily by asymptotic expansions, matching the *inner* solution, valid in the thin film region to the *outer* solution of the meniscus region. This can be done in a very similar fashion for both, the power-law model and the Ellis model.

**Power-law model** In the *inner* region the surface tension and flux terms, i.e. the term on the left of (4.5) and the last term on the right side of (4.5) must balance. This is achieved via the *inner scaling*

$$x = \varepsilon^\beta \xi, \quad h = \varepsilon^{\frac{3\beta}{n+2}} \phi, \quad h_\infty = \varepsilon^{\frac{3\beta}{n+2}} \Theta \quad (5.1)$$

Note here, that unlike the Newtonian case  $\beta$  is not known at this point and has to be determined by matching to the outer solution. Assuming the solutions have the asymptotic expansions

$$\phi(\xi; \varepsilon) = \phi_0(\xi) + \varepsilon \phi_1(\xi) + O(\varepsilon^2), \quad \Theta(\varepsilon) = \Theta_0 + \varepsilon \Theta_1 + O(\varepsilon^2) \quad (5.2)$$

we find for the leading order inner problem

$$\phi_0^{2n+1} \phi_0''' = -a^n (\phi_0 - \Theta_0)^n \quad (5.3)$$

where  $' = \partial_\xi$ . Clearly, in the limit as  $\xi \rightarrow \infty$  the solution will tend to the uniform thickness  $\phi_0 \rightarrow \Theta_0$ . The behavior towards the meniscus region can be found to have form

$$\phi_0(\xi) = A(n) \left( \frac{a^n}{\Theta_0^{n+2}} \right)^{\frac{2}{3}} \Theta_0 \xi^2, \quad \text{as } \xi \rightarrow -\infty \quad (5.4)$$

where the constants have to be matched by the solution of the *outer* problem, valid in the meniscus and  $A(n)$  is determined by the numerical solution of the (5.3). The *outer scaling* is given by

$$x = \varepsilon^{-\frac{1}{2}} \chi, \quad \text{and} \quad h = \varepsilon^{-\frac{3}{2}} \Phi \quad (5.5)$$

Hence, the outer problem is simply

$$\frac{d}{d\chi} \left( \frac{\Phi_{\chi\chi}}{(1 + \Phi_\chi^2)^{\frac{3}{2}}} \right) = 1. \quad (5.6)$$

which behaves as

$$\Phi(\chi) = \frac{\sqrt{2}}{2} \chi^2 \quad \text{as } \chi \rightarrow 0 \quad (5.7)$$



Written in inner coordinates yields

$$\phi_0(\xi) = \varepsilon^s \frac{\sqrt{2}}{2} \xi^2, \quad \text{where} \quad s = 2\beta + 1 - \frac{3}{2} - \frac{3\beta}{n+2} \quad (5.8)$$

But in order to match to (5.4)  $s$  must be zero. Therefore, matching yields the yet unknown scaling factor

$$\beta = \frac{n+2}{4n+2} \quad (5.9)$$

Furthermore, matching the coefficients yields

$$\Theta_0 = \left( \frac{2n+1}{n} \right)^{\frac{2n}{2n+1}} \left( \sqrt{2} A(n) \right)^{\frac{3}{2n+1}} \quad (5.10)$$

Since  $h_\infty = \varepsilon^{\frac{3}{4n+2}} \Theta_0$ , we finally obtain for the film thickness

$$h_\infty = \varepsilon^{\frac{3}{4n+2}} \left( \frac{2n+1}{n} \right)^{\frac{2n}{2n+1}} \left( \sqrt{2} A(n) \right)^{\frac{3}{2n+1}}. \quad (5.11)$$

**Ellis model** Here, the *inner scaling* is achieved by setting

$$x = \varepsilon^\alpha \xi, \quad h = \varepsilon^{\frac{3\alpha q}{2q+1}} \phi, \quad h_\infty = \varepsilon^{\frac{3\alpha q}{2q+1}} \Theta \quad (5.12)$$

which is the scaling that balances the second term of the left hand side of equation

$$\frac{1}{2} \left[ 1 + \frac{3}{q+2} \left( \frac{h}{E} \right)^{q-1} |\psi|^{q-1} \right] h^3 \psi = -3(h-h_\infty) + \frac{h_\infty^3}{2} \left[ 1 + \frac{3}{q+2} \left( \frac{h_\infty}{E} \right)^{q-1} \right] \quad (5.13)$$

with the first term on the right hand side. As is the power-law case, the exponent  $\alpha$  is yet unknown and has to be determined by matching to the outer solution. Additionally, we note that the balance of the first term on the left hand side would lead to the scaling for the Newtonian case, and a balance where both terms balance the first term on the right hand side leads to inconsistencies.

Assuming asymptotic expansions as in (5.2) we now find with the scaling (5.12) to leading order the *inner* problem

$$\frac{E^{1-q}}{2(q+2)} \phi_0^{q+2} \phi_0''' |\phi_0'''|^{q-1} = -(\phi_0 - \Theta_0) \quad (5.14)$$

Since  $\phi_0 - \Theta_0 > 0$  and  $\phi_0 > 0$  this equation can be written as

$$\phi_0^{q+2} \phi_0''' = -(\phi_0 - \Theta_0)^{\frac{1}{q}} \phi_0^{\frac{(q-1)(q+2)}{q}} \left( \frac{2(q+2)}{E^{1-q}} \right)^{\frac{1}{q}}. \quad (5.15)$$

Its solution attains the form

$$\phi_0 = C(q) \left( \frac{2(q+2)}{E^{1-q} \Theta_0^{2q+1}} \right)^{\frac{2}{3q}} \Theta_0 \xi^2 \quad \text{as} \quad \xi \rightarrow -\infty \quad (5.16)$$

The *outer* problem is the same as before, i.e. given by (5.5)–(5.7). Matching with (5.16) yields

$$\alpha = \frac{1}{2} \frac{2q+1}{q+2} \quad (5.17)$$

Solving for  $h_\infty$ , we find

$$h_\infty = \varepsilon^{\frac{3}{2} \frac{q}{q+2}} \left( C(q) \sqrt{2} \right)^{\frac{3q}{q+2}} \frac{(2(q+2))^{\frac{2}{q+2}}}{E^{\frac{2(1-q)}{q+2}}} \quad (5.18)$$

where again,  $C(q)$  is found by solving (5.15). Note that in both cases, higher order corrections can now in principle be carried out, as demonstrated in [22] for the Newtonian case, but one needs to ensure that no contributions neglected in the approximation leading to the governing equation (3.15) together with (4.4) and (2.4) will become important.

## 5.2 Comparison with numerical results

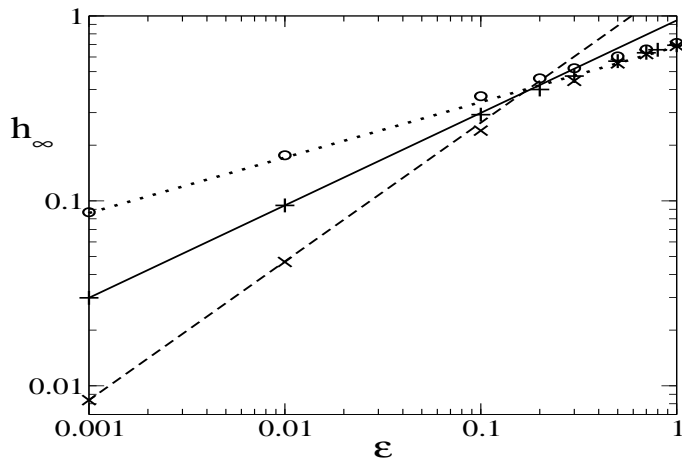


Figure 4: Comparison of the Type I meniscus film thicknesses for the power-law model obtained from the numerical solution of the steady state equation (symbols) and the asymptotic formula (lines). Shown are the results for three different values of the power law exponent,  $n = 0.5$  (— and  $\times$ ),  $n = 1$  (— and  $+$ ) and  $n = 2$  ( $\cdots$  and  $\circ$ ).

We rewrite asymptotic expressions for the Type I meniscus solution's film thickness obtained (5.11) for the Power-Law and in (5.18) for the Ellis-model to group the coefficients that only depend on  $n$  or  $q$ , respectively. We obtain, respectively,

$$h_\infty^{PL} = \tilde{A}(n) \varepsilon^{\frac{3}{4n+2}} \quad (5.19a)$$

with

$$\tilde{A}(n) = \left( \frac{2n+1}{n} \right)^{\frac{2n}{2n+1}} \left( \sqrt{2} A(n) \right)^{\frac{3}{2n+1}}, \quad (5.19b)$$

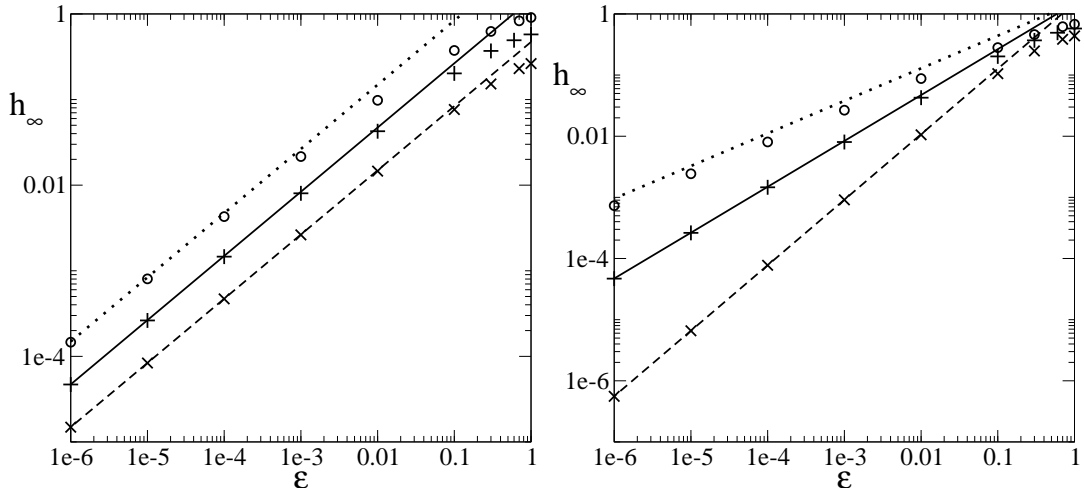


Figure 5: Comparison of the Type I meniscus film thicknesses for the power-law model obtained from the numerical solution of the steady state equation (symbols) and the asymptotic formula (lines). In (a), left, results are shown for fixed  $q = 2$  and three different values of  $E$ ,  $E = 0.05$  (— and  $\times$ ),  $E = 0.5$  (— and  $+$ ) and  $E = 5$  ( $\cdots$  and  $\circ$ ). In (b), right, results are shown for fixed  $E = 0.5$  and three different values of  $q$ ,  $q = 5$  (— and  $\times$ ),  $q = 2$  (— and  $+$ ) and  $q = 1.1$  ( $\cdots$  and  $\circ$ ).

and

$$h_{\infty}^E = \tilde{C}(q) E^{-\frac{2(1-q)}{q+2}} \epsilon^{\frac{3}{2} \frac{q}{q+2}}, \quad (5.20a)$$

with

$$\tilde{C}(q) = \left( C(q) \sqrt{2} \right)^{\frac{3q}{q+2}} (2(q+2))^{\frac{2}{q+2}}. \quad (5.20b)$$

We determined  $A(n)$  and  $C(q)$  by solving the appropriate inner problem numerically. For large negative values of  $-x$ , the second derivative of the solution with respect to  $x$  converges to a constant value, which is twice  $A(n)$  or  $C(q)$ , for the Power-Law or the Ellis model, respectively. From these, we obtain the values for  $\tilde{A}(n)$  and  $\tilde{C}(q)$  collected in the following table:

$n$	0.5	1	2	$q$	1.1	2	5
$\tilde{A}(n)$	1.488	0.9458	0.6826	$\tilde{C}(q)$	1.565	2.105	3.305

We now compare the film thicknesses computed from the asymptotic formulae (5.19a) and (5.20a) with the values of  $h_{\infty} = h_B$  for which a Type I meniscus solution was obtained numerically for the steady state equations.

For the power-law model, the results are shown in figure 4. For all three values of  $n$ , the asymptotic and the numerical solution agree quite well up to values of  $\epsilon$  near and above 0.1. Smaller values of  $n$  seem to lead to better agreement, which might have been expected since for larger  $n$ , smaller powers of  $\epsilon$  appear in the asymptotic expansions for  $h_{\infty}$ , suggesting that higher corrections have a stronger impact.

For the Ellis model, we first fix  $q = 2$  and vary  $E$  over two orders of magnitude. The agreement is good, upto  $\epsilon = 0.1$  for the  $E = 0.5$  and  $E = 5$  case and to a somewhat lesser extent for  $E = 50$ . For the leading order result (5.20a), increasing  $E$  increases the coefficient and if this is the case also for the coefficients in the next corrections, this could explain why the agreement deteriorates for larger  $E$ .

Next, we keeps  $B = 0.5$  fixed and vary  $q$ . Agreement is good up to  $\epsilon = 0.1$  for  $q = 2$  and  $q = 5$ , however, for  $q = 1.1$ , there is a notable though decreasing discrepancy even down to values of  $10^{-6}$  for  $\epsilon$ . The reason for this can be easily seen from the asymptotics: The dominant terms of the steady state problem (5.13) for the Ellis model in inner scales and the neglected term on the left hand side become of same order as  $q \rightarrow 1$  from above.

## Conclusions

In this study we derived lubrication models for the drag-out problem at variable inclination angle for some of the most popular viscosity models from the underlying free boundary problem governed by the equations of momentum and mass conservation. A system of ordinary differential equations for the steady states, that is obtained from the lubrication equations is investigated using phase plane analysis. This yields criteria for the possibility of Type I, corresponding to the monotone meniscus profile and Type II, corresponding to the spatially oscillating meniscus profile, as a function of the rheological parameters. It would be interesting to compare our findings with experimental results and further explore the relevant parameters that control the shape of the free boundary, in particular in view of the implications for many related problems, such as the well-known Bretherton problem [7] or the roller-coating problem. We note that it is clear from our work that it is straight forward to generalize our analysis also to the three-dimensional case.

## Appendix 1

### Lubrication equation for the Ellis model

As before we balance in the  $x$ -momentum equation  $p_x$  with the dominant viscous stress term  $\tau_z^{xz}$ . Then

$$P = \frac{\eta_0 U}{2\epsilon H}$$

Balancing  $\tau_z^{xz}$  in the  $x$ -momentum equation with the gravity term yields

$$H = \left( \frac{\eta_0 U}{2\rho g \cos \alpha} \right)^{\frac{1}{2}}$$

We introduce here the dimensionless viscosity by

$$\bar{\eta} = \frac{\eta_0}{2}\eta$$

where

$$\frac{\eta_0}{\bar{\eta}} = 1 + \left| \frac{\bar{\tau}}{\tau_{\frac{1}{2}}} \right|^{q-1}$$

Hence,

$$\frac{2}{\eta} = 1 + \left( \frac{\eta_0 U}{2H\tau_{\frac{1}{2}}} \right)^{q-1} |\tau^{xz}|^{q-1}$$

The leading order dimensionless equations are (3.6a)-(3.7b) where  $\tau^{zx} = -\eta u_z$ . These can be integrated to yield the expression for the component of the stress tensor

$$\tau^{xz} = -\psi(x, t)(h - z),$$

which can now be used to derive an expression for the velocity, since  $\eta u_z = \psi(h - z)$ . Hence,

$$u_z = \psi \frac{h - z}{\eta} = \frac{1}{2} \psi(h - z) \left( 1 + \frac{|\tau^{xz}|^{q-1}}{E^{q-1}} \right) = \frac{1}{2} \psi(h - z) \left( 1 + \frac{|\psi|^{q-1} |h - z|^{q-1}}{E^{q-1}} \right)$$

We assume  $h > z$  and get

$$u_z = \frac{1}{2} \left( \psi(h - z) + \frac{\psi |\psi|^{q-1} (h - z)^q}{E^{q-1}} \right)$$

Integrating this w.r.t.  $z$  and using the no-slip condition, we find

$$u = \frac{1}{2} \left[ \psi(hz - z^2) + \frac{\psi |\psi|^{q-1}}{E^{q-1}} \left( \frac{-1}{q+1} (h - z)^{q+1} + \frac{1}{q+1} h^{q+1} \right) \right] + 1$$

Hence, we get for the flux

$$\begin{aligned} Q &= \int_0^h u \, dz \\ &= \frac{1}{2} \left[ \psi(hz - z^2) \Big|_0^h + \frac{\psi |\psi|^{q-1}}{E^{q-1}} \left( \frac{1}{(q+1)(q+2)} (h - z)^{q+2} + \frac{1}{q+1} h^{q+1} z \right) \Big|_0^h + z \Big|_0^h \right] \\ &= \frac{1}{2} \left[ \psi \left( \frac{h^3}{2} - \frac{h^3}{6} \right) + \frac{\psi |\psi|^{q-1}}{E^{q-1}} \left( \frac{1}{(q+1)} h^{q+2} + \frac{1}{(q+1)(q+2)} h^{q+2} \right) \right] + h \end{aligned}$$

Therefore we get

$$Q = \int_0^h u \, dz = \frac{1}{2} \left[ \psi \frac{h^3}{3} + \frac{\psi |\psi|^{q-1}}{E^{q-1}} \frac{h^{q+2}}{q+2} \right] + h$$

which we plug into the kinematic condition to obtain the lubrication equation

Using the time scaling  $t \rightarrow 3t$  we get finally the following lubrication equation for the Ellis model

$$\partial_t h = -\partial_x \left[ \frac{1}{2} \left( \psi h^3 + \frac{3}{q+2} \frac{1}{E^{q-1}} \psi |\psi|^{q-1} h^{q+2} \right) + 3h \right]$$

where we rescaled time as  $t \rightarrow 3t$ .

## Appendix 2

### Lubrication equation for the Carreau model

Again we non-dimensionalize as before and assume additionally that the new parameter  $\lambda$  is scaled as

$$\bar{\lambda} = \lambda T = \lambda^* \varepsilon T$$

i.e.  $\lambda = O(1/\varepsilon)$  and  $\lambda^* = O(1)$ . Hence,

$$\eta = \eta_0 \left[ 1 + \left( \frac{\lambda \dot{\gamma}}{\varepsilon} \right)^c \right]^{\frac{k-1}{c}} = \eta_0 [1 + (\lambda^* \dot{\gamma})^c]^{\frac{k-1}{c}}$$

and the shear stress components are

$$\begin{aligned} \bar{\tau}^{xx} &= -\frac{\eta_0 U}{H} \varepsilon^2 u_x [1 + (\lambda \dot{\gamma})^c]^{\frac{k-1}{c}}, \\ \bar{\tau}^{xz} &= -\frac{\eta_0 U}{H} (u_z + \varepsilon^2 w_x) [1 + (\lambda \dot{\gamma})^c]^{\frac{k-1}{c}}, \\ \bar{\tau}^{zz} &= -\frac{\eta_0 U}{H} \varepsilon^2 w_z [1 + (\lambda \dot{\gamma})^c]^{\frac{k-1}{c}}, \end{aligned}$$

Integrating the system (3.6a)-(3.7b) once w.r.t.  $z$  we find

$$u_z (1 + |\lambda^* u_z|^c)^{\frac{k-1}{c}} = \psi(x, t)(h - z)$$

If we define

$$\omega := |\lambda^* u_z|^c, \quad \text{and} \quad g(x, z, t) := (\lambda^* |\psi|(h - z))^c$$

we obtain the equation

$$\omega(1 + \omega)^{k-1} = g$$

and

$$u_z = \frac{\psi(h - z)}{(1 + \omega(g))^{\frac{k-1}{c}}}.$$

Upon integrating this once, it is convenient to change integration variables to  $\omega$ , via

$$dz = -\frac{g^{\frac{1-c}{c}}}{c\lambda^*|\psi|} dg \quad \text{and} \quad dg = \frac{1 + k\omega}{(1 + \omega)^{2-k}}$$

which leads to

$$u(x, z, t) = -\frac{F(\omega(g(z))) - F(\omega(g(0)))}{c\lambda^*2\psi} + 1$$

where

$$F(\omega) = \int \frac{\omega^{\frac{2-c}{c}}(1 + k\omega)}{(1 + \omega)^{\frac{1-k}{c}+1}} d\omega$$

To derive an expression for the flux involves the integral

$$\int_0^h [F(\omega(g(z))) - F(\omega(g(0)))] dz = -\frac{1}{c\lambda^*|\psi|} \int_{\omega_0}^0 (F(\omega) - F(\omega_0)) \frac{\omega^{\frac{1-c}{c}}(1 + k\omega)}{(1 + \omega)^{\frac{1-k}{c}+1}} d\omega$$

If we note that

$$\begin{aligned} \int_{\omega_0}^0 \frac{1+k\omega}{(1+\omega)^{\frac{3-k}{2}}} \omega^{1/2} d\omega &= -2\omega_0^{1/2} F_1 - \frac{2}{3} k\omega_0^{3/2} F_2 \\ - \int_{\omega_0}^0 \frac{1-k^2\omega^2}{(1+\omega)^{2-n}} \omega^{1/2} d\omega &= 2\omega_0^{1/2} F_3 - \frac{2}{5} k^2 \omega_0^{5/2} F_4 \end{aligned}$$

where

$$\begin{aligned} F_1 &= F\left(\frac{1}{2}, \frac{3-k}{2}; \frac{3}{2}; -\omega_0\right), & F_2 &= F\left(\frac{3-k}{2}, \frac{3}{2}; \frac{5}{2}; -\omega_0\right), \\ F_3 &= F\left(\frac{1}{2}, 2-k; \frac{3}{2}; -\omega_0\right), & F_4 &= F\left(\frac{5}{2}, 2-k; \frac{7}{2}; -\omega_0\right). \end{aligned}$$

Hence, we obtain for the flux

$$\begin{aligned} Q^C(x, t) &= \int_0^h u dz \\ &= \frac{\sqrt{\omega_0}}{\lambda^{*3}(k+1)\psi|\psi|} \frac{1}{\left(\omega_0+1\right)^{\frac{1-k}{2}}} \left[ \frac{k\omega_0-1}{\left(\omega_0+1\right)^{\frac{1-k}{2}}} \left( F_1 + \frac{k\omega_0}{3} F_2 \right) + \left( F_3 - \frac{k^2\omega_0^2}{5} F_4 \right) \right] + h \end{aligned}$$

and the corresponding lubrication equation

$$\partial_t h = -\partial_x Q^C$$

with boundary condition at  $x \rightarrow \pm\infty$

$$\begin{aligned} \lim_{x \rightarrow -\infty} h &= h_\infty, & \lim_{x \rightarrow -\infty} h_x &= 0, \\ \lim_{x \rightarrow \infty} \kappa &= 0, & \lim_{x \rightarrow \infty} h &= \infty. \end{aligned}$$

## References

- [1] M. Abramowitz and I. Stegun. *Handbook of Mathematical Functions*. Dover Publications Inc., New York, 1972.
- [2] A. Acrivos, M. J. Shan, and E. E. Petersen. On the flow of a non-newtonian liquid on a rotating disk. *J. Appl. Phys.*, 31:963–968, 1960.
- [3] K. Afanasiev, A. Münch, and B. Wagner. Thin film dynamics on vertically rotating disks. submitted to: *Applied Mathematical Modelling*, 2007.
- [4] V. I. Baikov, Z. P. Shul'man, and K. Engel'gardt. Coating of a non-newtonian fluid onto a moving surface. *Zhurnal Prikladnoi Mekhaniki i Tekhnicheskoi Fiziki*, 4:53–59, 1985.
- [5] A. L. Bertozzi, A. Münch, and M. Shearer. Undercompressive waves in driven thin film flow. *Physica D*, 134:431–464, 1999.

- [6] R. B. Bird, R. C. Armstrong, and O. Hassager. Dynamics of polymeric fluids. Vol.I, Fluid Mechanics, John Wiley and Sons, New York, 1977.
- [7] F. P. Bretherton. The motion of long gas bubbles in tubes. *J. Fluid Mech.*, 10:166–188, 1961.
- [8] J. A. Britten and I. M. Thomas. Non-newtonian flow effects during spin coating large-area optical coatings with colloidal suspensions. *J. Appl. Phys.*, 71:972–979, 1992.
- [9] L. W. S. D. E. Weidner. Contact-line motion of shear-thinning liquids. *Physics of Fluids*, 6:3535–3538, 1994.
- [10] S. Fomin, J. Watterson, S. Raghunathan, and E. Harkin-Jones. Steady-state rimming flow of the generalized newtonian fluid. *Physics of Fluids*, 14:3350–3353, 2002.
- [11] A. C. H. K. Radhakrishnan. Description and use of lsode: the livermore solver for ordinary differential equations. *Lawrence Livermore National Laboratory Report*, UCRL-ID-113855, 1993.
- [12] L. Landau and B. Levich. Dragging of a liquid by a moving plate. *Acta Physicochimica U.R.S.S*, 17(1):42–54, 1942.
- [13] C. J. Lawrence. The mechanics of spin coating of polymer films. *Phys. Fluids*, 31:2786–2795, 1988.
- [14] C. J. Lawrence and W. Zhou. Spin coating of non-newtonian fluids. *J. of Non-Newtonian Fluid Mechanics*, 39:137–187, 1991.
- [15] J. T. T. M. S. Christodoulou and S. Wilson. A model for the low to moderate speed performance of the rotating disk skimmer. *Journal of Fluids Engineering*, 112, 1990.
- [16] S. Matsuhisa and R. B. Bird. Analytical and numerical solution for laminar flow of the non-newtonian ellis fluid. *AIChE Journal*, 11:588–595, 1965.
- [17] A. Münch. The thickness of a marangoni-driven thin liquid film emerging from a meniscus. *SIAP*, 62:2045–2063, 2002.
- [18] A. Münch and P. L. Evans. Marangoni-driven liquid films rising out of meniscus onto a nearly-horizontal substrate. *Physica D*, 209:164–177, 2005.
- [19] T. G. Myers. Application of non-newtonian models to the thin film flow. *Physical Review E*, 72:066302, 2005.
- [20] S. V. Nitta, A. Jain, P. Wayner, Jr., W. N. Gill, and J. L. Plawsky. Effect of sol rheology on the uniformity of spin-on silica xerogel films. *J. Appl. Phys.*, 86:5870, 1999.



- [21] L. W. Schwartz. On the asymptotic analysis of surface-stress-driven thin-layer flow. *J. Engrg. Math.*, 39:171, 2001.
- [22] S. D. R. Wilson. The drag-out problem in film coating theory. *J. Engg. Math.*, 16:209–221, 1982.